Indian Journal of Chemical Technology
Vol. 24, January 2017, pp. 61-66

Influence of 3-acetylpyridine phenylhydrazone on the corrosion of carbon steel in hydrochloric acid

Vinod P Raphael, Joby Thomas K*, Shaju K S & Nimmy Kuriakose

Research Division, Department of Chemistry, St. Thomas' College, (University of Calicut) Thrissur 680 001, Kerala, India
E-mail: drjobythomask@gmail.com

Received 29 October 2014; accepted 25 August 2015

The corrosion inhibition capacity of the 3-acetylpyridine phenylhydrazone (APPH) has been investigated by gravimetric studies and electrochemical investigations like EIS and Tafel polarization analyses. Present study reveal that APPH act as a potential corrosion inhibitor on carbon steel even when the molecules are hydrolyzed in acid medium. Polarization studies establish that the molecule show mixed type corrosion inhibition on CS surface. Results obtained from these techniques are comparable and the hydrazone obey Langmuir adsorption isotherm on the corroding metal surface. Thermodynamic parameters of corrosion such as activation energy (E_a), enthalpy and entropy of activation of corrosion (ΔH^* and ΔS^*) have also been estimated. Surface analysis using AFM confirm the adsorption of APPH molecules on the metal surface.

Keywords: Carbon steel, Phenylhydrazone, Corrosion inhibitors, Isotherm, AFM

The enormous use of acid in various industrial processes such as de-scaling, pickling, oil well acidizing etc will enhance the rate of corrosion of metals significantly. The addition of corrosion inhibitors into the acidic medium is indispensible to reduce the metallic dissolution. Several heterocyclic organic molecules and imines act as corrosion inhibitors in acidic media[1-3]. The hetero atoms like O, N, S and azomethine linkage act as potential sites for corrosion inhibition for carbon steel, aluminum, copper and zinc in acidic media[4-11]. The present investigation focussed on the corrosion inhibition competence of 3-acetylpyridine phenylhydrazone (APPH) on carbon steel (CS) in 1.0 M HCl with the aid of gravimetric and electrochemical studies.

Experimental Section

Synthesis

APPH was synthesized by the reaction between equimolar mixture of 3-acetylpyridine in ethanol and phenylhydrazine hydrochloride in ethanol water mixture (3:1). The reaction mixture was refluxed for four hours and evaporated near to dryness and cooled slowly. The precipitated yellow coloured compound was filtered, washed with small quantity of ethanol and recrystallised from ethanol. m.p. = 245°C.

Metal specimen and aggressive medium

Carbon steel coupons containing 0.58% Mn, 0.07% P, 0.02% S, 0.015% Si, 0.02% and the rest Fe (determined by EDAX method) were cut and mechanically abraded with various grades of silicon carbide papers (120, 400, 600, 800, 1000 and 1200). The surface area of the metal specimens was accurately determined, washed and degreased with acetone, and weighed. A stock solution of the APPH (1.0 mM in 1.0 M HCl) diluted with 1.0 M HCl acted as inhibitor solutions having concentrations 0.2-1.0 mM.

Gravimetric corrosion studies

Well polished CS specimens were immersed in aggressive solutions having different concentrations of the APPH for 24 h. A blank experiment was also conducted without APPH. The weight loss occurred for metal specimens were measured after 24 h. To ensure good reproducibility, all experiments were carried out in duplicate and the average values were taken. The corrosion rate was calculated by the following equation[8,12].

$$\upsilon = \frac{KW}{DST} \quad \text{... (1)}$$

where, υ = corrosion rate (mmy^{-1}), W = weight loss (g), S = surface area of metal specimen (cm^2), t = time

of treatment (h), D = density of specimen (gcm^{-3}) and K = a constant (8.76×10^4).

Percentage of inhibition or the inhibition efficiency[13] (η) was obtained by the Eq 2.

$$\eta = \frac{\upsilon - \upsilon'}{\upsilon} \times 100 \quad \text{... (2)}$$

where υ and υ' are the corrosion rate of the CS specimen in the absence and presence of the APPH respectively.

Effect of temperature on corrosion

The effect of temperature on corrosion was evaluated by the weight loss studies in the temperature range 30-60°C. The activation energy of corrosion with and without APPH was calculated by Arrhenius equation[14],

$$\boldsymbol{K} = \boldsymbol{A}\exp\left(-\frac{\boldsymbol{Ea}}{\boldsymbol{RT}}\right) \quad \text{... (3)}$$

where $\boldsymbol{K}$ is the rate of corrosion, $\boldsymbol{E}_a$ the activation energy, A the frequency factor, T the temperature in Kelvin scale and R is the gas constant. Arrhenius curves were obtained by plotting logK against 1000/T. Enthalpy and entropy of activation (ΔH*, ΔS*) were calculated from the transition state theory, which can be represented by the following equation[14].

$$\boldsymbol{K} = \left(\frac{\boldsymbol{RT}}{\boldsymbol{Nh}}\right)\exp\left(\frac{\Delta \boldsymbol{S}^*}{\boldsymbol{R}}\right)\exp\left(\frac{\Delta \boldsymbol{H}^*}{\boldsymbol{RT}}\right) \quad \text{... (4)}$$

where N is the Avogadro number and h is the Planks constant.

Electrochemical corrosion investigations

The electrolytic cell was a cubical glass vessel containing two openings. Two electrodes namely saturated calomel (reference) and platinum electrode having $1cm^2$ surface area were inserted from the top. The working electrode was CS strip in which the $1cm^2$ area of the strip was exposed to the solution through the second opening. All potentials were measured with reference to SCE. In order to avoid the effects of polarization, the reference electrode and the working electrode were kept so close. Before each experiment, the working electrode surface was polished using SiC papers of various grades, cleaned and degreased. Ivium compactstat-e electrochemical system together with Iviumsoft software package was employed to perform the experiments.

Potentiodynamic polarization studies were performed between +100 to -100mV with a sweep rate of 1mV/s. Slope analysis of Tafel curves gave the corrosion current densities and the inhibition efficiency was calculated by the following equation[15].

$$\eta pol\,\% = \frac{I_{corr} - I_{corr}}{I_{Corr}} \times 100 \quad \text{.. (5)}$$

where I_{corr} and I'_{corr} are uninhibited and inhibited corrosion current densities respectively.

Electrochemical impedance spectroscopic studies were also performed to monitor the corrosion inhibition efficacy. Constant potential (OCP) in the frequency range from 1 KHz to 100 mHz with an amplitude of 10 mV as excitation signal was employed for every experiment. From the charge transfer resistance obtained by the analysis of Nyquist and Bode plots, corrosion inhibition efficiency was calculated by the following equation[2].

$$\eta_{EIS}\,\% = \frac{R_{ct} - R_{ct}}{R_{ct}} \times 100 \quad \text{... (6)}$$

where R_{ct} and R'_{ct} are the charge transfer resistances of working electrode with and without inhibitor, respectively.

AFM studies

Surface topography of the metal specimens was studied by AFM (Park Systems XE-100 model) in contact mode. The surface micrographs were recorded by scanning 5 μm × 5 μm area at a scan rate of 0.8 Hz.

Results and Discussion

Characterization of APPH

Base peak in the mass spectrum was observed at ***m/z***: 211(molecular mass). Signals appeared at 92, 78, 65 and 51 were due to the fragments $[C_6H_6N]^+$, $[C_5H_4N]^+$, $[C_5H_5]^+$ and $[C_4H_3]^+$. Anal. calcd for $C_{13}H_{13}N_3$: C, 73.93; H, 6.16; N, 19.9%. Found: C, 73.47; H, 6.42; N, 19.44%. In the IR spectrum, $\upsilon_{C=N}$ and υ_{N-H} appeared at 1593 and 3265 cm^{-1} respectively. Electronic transitions occurred in the molecules were observed at 32679 and 29239 cm^{-1}, which were due to $\pi\rightarrow\pi^*$ and $n\rightarrow\pi^*$ transitions respectively. Figure 1 shows the optimized geometry of APPH.

Gravimetric studies

The rate of CS corrosion in 1.0 M HCl was 6.54 mmy^{-1}. Table 1 represents the corrosion inhibition efficiencies (%) of the heterocyclic

phenylhydrazone APPH on CS in HCl. The corrosion rate of the carbon steel in hydrochloric acid medium was noticeably decreased in the presence of APPH. Even at low concentrations, this compound inhibited the metallic dissolution appreciably in the acidic medium. From Table 1 it is evident that inhibition capacity escalated with the inhibitor concentration.

The remarkable corrosion preventing ability of this molecule may be attributed to the presence of highly delocalized π electron cloud of the benzene ring, hetero nitrogen atom and azomethine group. It was confirmed by UV-visible spectral study that APPH undergo slow hydrolysis into their parent compounds in acidic medium. Gravimetric corrosion studies were also performed by choosing the parent ketone, 3-acetylpyridine (3AP) and parent amine, phenyl hydrazine (PH) and their equimolar mixture as the test compounds in acidic medium (Table 1). Results revealed that the parent compounds were scarcely inhibitive than hydrazone. One may conclude that the APPH molecules which were directly attached to the metal surface through the chloride ion did not undergo hydrolysis. In continuation to our research work, we could establish the corrosion antagonistic behaviour (accelerating corrosion with concentration) of APPH in 0.5 M sulphuric acid on CS due to the intensive hydrolysis. But this molecule displayed very high inhibition efficiency in the presence of trace of iodide ions due to the formation of strong protective film[16]. The reluctance to hydrolysis of the adsorbed APPH molecules which are strongly attached on the metal surface through halide ions is thus well established by these investigations.

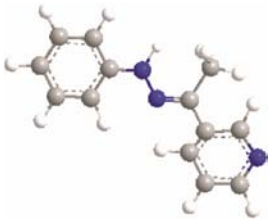

Fig. 1 — Optimized geometry of APPH

Table 1 — Gravimetric corrosion inhibition efficiencies of various systems on CS for 24 h

C (mM)	APPH	3AP	PH	3AP+PH
0.2	85.63	55.43	58.45	62.3
0.4	88.80	-	-	-
0.6	89.26	67.78	61.24	64.90
0.8	90.34	-	-	-
1.0	91.47	69.92	68.74	72.30

The most expedient mode of expressing adsorption quantitatively is to originate the adsorption isotherm that characterizes the metal/inhibitor/ environment system. Attempts were made to fit θ values to various adsorption isotherms with the aid of correlation coefficient. Langmuir adsorption isotherm (Eq. 7) fits well the experimental data for APPH on CS surface.

$$\frac{C}{\theta} = \frac{1}{Kads} + C \qquad \ldots (7)$$

where C is the concentration of the inhibitor, θ is the fractional surface coverage and K_{ads} is the adsorption equilibrium constant[17]. It is well known that the standard free energy of adsorption ($\Delta G°_{ads}$) is related to equilibrium constant of adsorption (K_{ads}) by the following equation

$$\Delta G^0_{ads} = -RT\ln(55.5\ K_{ads}) \qquad \ldots (8)$$

where 55.5 is the molar concentration of water, R is the universal gas constant and T is the temperature in Kelvin[18]. For the adsorption of APPH on CS surface, K_{ads} and ΔG_{ads} were 48356 and -37.04 $kJmol^{-1}$ respectively, indicating a very strong interaction of APPH on CS surface, mainly through chemisorption[19,20].

Effect of temperature

Regression coefficients of Arrhenius and other thermodynamic plots were close to unity indicating that the corrosion of CS in HCl can be explained by the simple kinetic model. Table 2 explores the activation energy and thermodynamic parameters of corrosion of CS in 1.0 M HCl in the presence and absence of APPH.

It is apparent from the results that activation energy of dissolution of metal increased with APPH concentration. This implies that the reluctance of

Table 2 — Thermodynamic parameters of corrosion of CS in the presence and absence of APPH in 1.0 M HCl

C (mM)	E_a (kJ mol^{-1})	A	ΔH* (kJ mol^{-1})	ΔS* (J mol^{-1} K^{-1})
Blank	32.86	2.76×10^6	30.21	-100.88
0.2	73.73	4.68×10^{12}	71.10	-11.14
0.4	80.5	5.37×10^{13}	77.90	8.99
0.6	83.61	1.58×10^{14}	81.01	17.99
0.8	87.02	5.01×10^{14}	84.41	27.57
1.0	93.17	4.27×10^{15}	90.50	45.38

dissolution of metal increased with the inhibitor concentration, which can be attributed to the considerable intervention of APPH molecules during the metallic dissolution. Positive signs of enthalpies with a regular rise reflect the endothermic nature of corrosion and the increasing difficulty for dissolution with the inhibitor strength. It is also evident from the thermodynamic data that the entropy of activation increased with APPH concentration. In the absence, as well as in low concentration of APPH (0.2 mM), ΔS^* exhibited negative values. This suggests that in the rate determining step, activated molecules were in higher order state than that at the initial state. As the concentration of APPH goes up, the disordering of activated complex increases and the entropy of activation attains positive values.

Electrochemical corrosion studies

The phenylhydrazone APPH displayed higher inhibitive action on CS surface according to Tafel polarization studies (Table 3). The corrosion current densities decreased significantly with the concentration of APPH. At all levels of investigations, the cathodic slopes b_c and anodic slopes b_a of the Tafel curves (Fig. 2) were affected. Besides, the E_{corr} values with respect to the blank experiment didn't alter considerably (maximum shift 22). Hence APPH is believed to behave as mixed type inhibitor[21,22].

Nyquist and Bode plots recorded for CS electrode in 1.0 M HCl solution and containing various concentrations of APPH are shown in Figs 3a and 3b respectively. Nyquist plots did not demonstrate ideal semicircles as predicted by the EIS theory. This deviation can be attributed to the frequency dispersion as well as the non homogeneity of the metal surface and mass transport resistance[23-26].

The analysis of Nyquist plots from experimental data was done by the most suitable equivalent circuit i.e., Randles circuit (inset in Fig. 3a), in which R_s represents the electrolyte resistance, R_{ct} represents the charge transfer resistance and C_{dl} the constant phase element[27,28]. Nyquist plots showed that the impedance behaviour of CS has significantly altered by the addition of APPH to the corrodent. R_{ct} values were higher than the uninhibited one and the impedance of inhibited systems were increased with increasing concentration of APPH molecules in HCl. Since the adsorbed molecules displace water molecules and other ions initially adsorbed on the metal surface, the electrical capacity should have decreased with the concentration of APPH. The modified adsorbed layer by the organic molecules builds a barrier for mass and charge transfers. The EIS parameters such as charge transfer resistance (R_{ct}) and double layer capacitance (C_{dl}) and the percentage of inhibition efficiencies are depicted in Table 3.

AFM analysis

To confirm the surface interaction of the heterocyclic phenylhydrazone on CS, AFM studies were performed. The three dimensional topography of bare metal, blank metal and metal specimen immersed in 1.0 M HCl along with 1.0 mM APPH for 24 h are given in Figs 4a, 4b and 4c respectively.

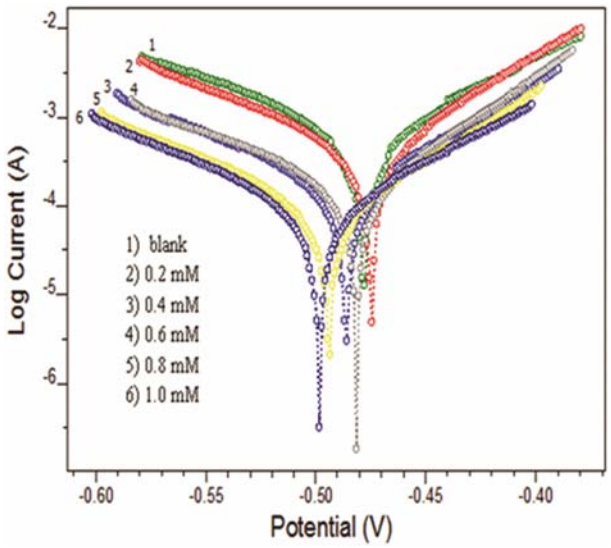

Fig. 2 —Tafel plots of CS in the presence and absence of APPH in 1.0 M HCl

Table 3—Polarization and impedance data of CS in the presence and absence of APPH in 1.0 M HCl

C (mM)	E_{corr} (mV/SCE)	I_{corr} ($\mu A/cm^2$)	$-b_c$ (mV/dec)	b_a(mV/dec)	$\eta_{pol\%}$	R_{ct} (Ωcm^2)	C_{dl} ($\mu F\ cm^{-2}$)	$\eta_{EIS\%}$
0	-474	499.6	102	77	-	23.08	76.36	-
0.2	-472	130.18	101	62	73.94	85.01	54.3	72.85
0.4	-486	89.92	100	69	82.00	166.24	45.87	86.11
0.6	-477	60.88	111	61	87.81	177.18	43.45	86.92
0.8	-490	49.01	97	69	90.19	369.2	43.11	93.70
1.0	-496	35.59	95	75	92.87	599.44	40.28	96.14

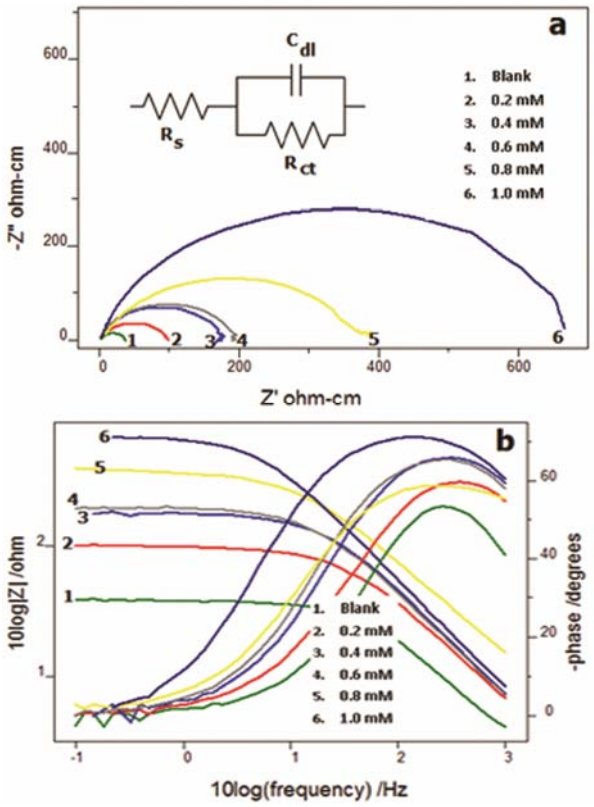

Fig. 3 — a) Nyquist plots and b) Bode plots of CS in the presence and absence of APPH in 1.0 M HCl

The roughness parameters that characterize the topography of surfaces like average roughness (arithmetic mean of the absolute values of the height of the surface profile, R_a), root mean square roughness (mean squared absolute values of surface roughness profile R_q), ten point roughness (arithmetic mean of the five highest peaks added to the five deepest valleys over the evaluation length measured R_z) and maximum peak to valley height (R_{px})[29,30] are provided in Table 4.

For the polished carbon steel surface (bare metal), the roughness parameters were very low when compared to blank metal specimen treated with 1.0 M HCl. It may be due to the atmospheric corrosion and the effect of polishing which caused the bare metal to show slight roughness in the AFM topography. The average roughness R_a and other parameters were significantly higher in the case of blank CS specimen. Examination of the topography of the metal immersed in 1.0 M HCl for 24 h, evidently proclaim that the surface was severely corroded by the attack of acid. On the addition of the APPH molecules to HCl, it can be assured that the molecules adhered on the metal surface with considerable strength protect the metal from corrosion. Topography of the metal in the presence of APPH showed smoother regions

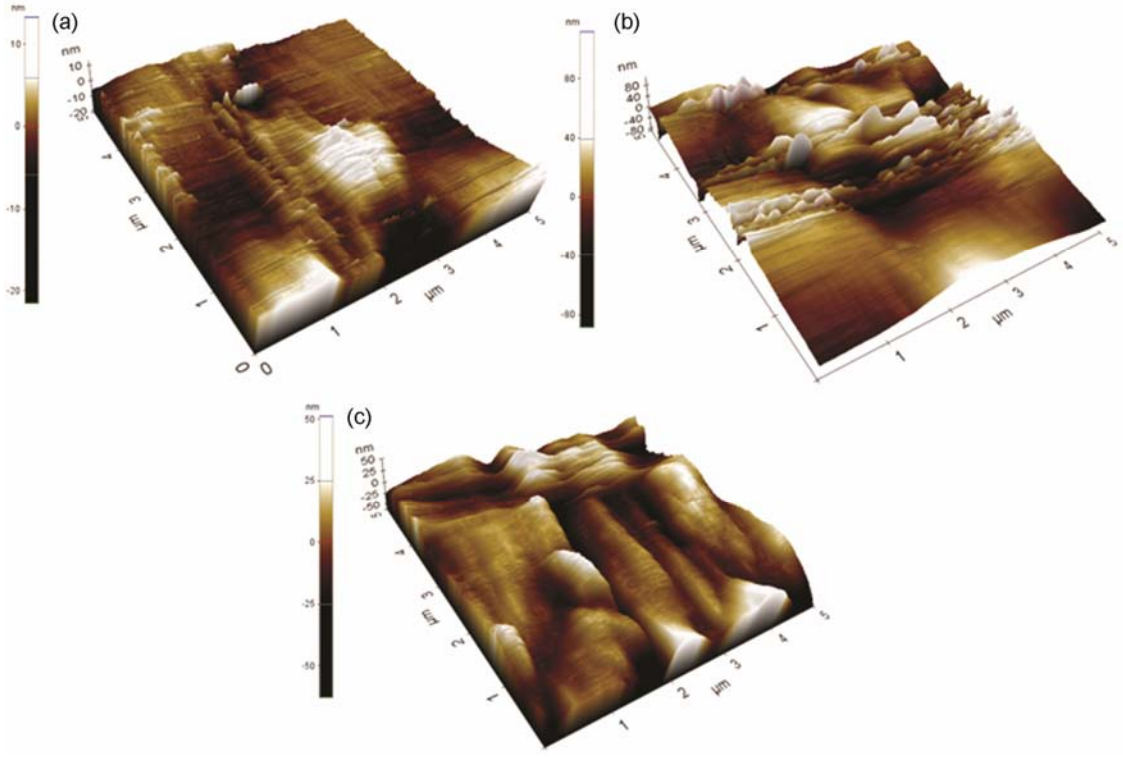

Fig. 4 — Topography of a) bare metal; b) metal treated with 1.0 M HCl for 24 h; c) metal treated with 1.0 M HCl and 1.0 mM APPH for 24 h

Table 4 — Roughness parameters of metal specimens by AFM studies

Metal surface	Peak -to- valley height R_{px} (nm)	RMS roughness R_q (nm)	Average roughness R_a (nm)	Ten point roughness R_z (nm)
Bare metal	34.79	3.02	2.16	30.66
Metal in 1.0 M HCl (24 h)	200.34	20.07	15.68	171.0
Metal in 1.0M HCl with 1.0 mM APPH (24h)	113.87	12.74	8.55	107.01

and the roughness parameters were significantly lowered when compared to the CS surface immersed in 1.0 M HCl.

Conclusion

Evaluating the results of corrosion monitoring techniques led to the following conclusions

- APPH exhibit outstanding corrosion inhibition efficiency on carbon steel in HCl.
- Even though APPH is susceptible to hydrolysis, the molecules which are making protective layer through chloride ions on steel surface didn't undergo decomposition.
- APPH obey Langmuir adsorption isotherm on CS surface in HCl and the interaction between the metal and APPH is mainly chemical in nature.
- Evaluation of the thermodynamic parameters clearly justifies the APPH-metal interaction.
- EIS measurements depict that declining of double layer capacitance and increasing of charge transfer resistance with concentration are the evidences for the adsorption of APPH molecules on the steel surface.
- By assessing the polarization parameters, the mixed inhibiting nature of the APPH has been established.
- Topographical studies of the metal specimens using AFM reveals that APPH molecules are well adsorbed on the metal surface to reduce the rate of corrosion appreciably.

References

1 Bentiss F, Traisnel M, Gengembre L & Lagrenée M, ***Appl Surf Sci***, 161 (2000) 194.
2 Raman A & Labine P, ***Reviews on Corrosion Inhibitor Sci Technol***, Vol. 1, NACE, Houston, TX (1986).
3 Oguzie E E, ***Mater Lett***, 59 (2005) 1076.
4 Yurt A & Aykın O, ***Corros Sci***, 53 (2011) 3725.
5 Singh A K, Shukla S K, Singh M & Quraishi M A, ***Mater Chem Phy***, 129 (2011) 68.
6 Behpour M, Ghoreishi S M, Soltani N, Salavati-Niasari M, Hamadanian M & Gandomi A, ***Corros Sci***, 50 (2008) 2172.
7 Stanly J K & Parameswaran G, ***Corros Sci***, 52 (2010) 224.
8 Yadav M, Kumar S, Kumari N, Bahadur I & Ebenso E E, ***Int J Electrochem Sci***,10 (2015) 602.
9 Li X, Deng S & Fu H, ***Mater Chem Phy***, 129 (2011) 696.
10 ***Bansiwal*** A, ***Anthony P & Mathur S P, Br Corros J***, 35 (4) (2000) 301.
11 Li S, Chen S, Lei S, Ma H, Yu R & Liu D, ***Corros Sci***, 41 (1999) 1273.
12 AST G-31-72, ***Standard Recommended Practice for the Laboratory Immersion Corrosion Testing of Metals***, ASTM , Philadelphia, PA (1990).
13 John S & Joseph A, ***Indian J Chem Technol***, 19 (2012) 195.
14 Bouklah M, Benchat N, Hammouti B, Aouniti A & Kertit S, ***Mater Lett***, 60 (2006) 1901.
15 Ashassi-Sorkhabi H, Shaabani B & Seifzadeh D, ***Electrochim Acta***, 50 (2005) 3446.
16 Raphael V P, Kakkassery J T, Shanmughan S K & Paul A, ***ISRN Corrosion***, (2013) doi:10.1155/2013/390823.
17 Li X, Deng S, Fu H & Li T, ***Electrochim Acta***, 54 (2009) 4089.
18 Cano E, Polo J L, La Iglesia A & Bastidas J M, ***Adsorption***, 10 (2004) 219.
19 Bentiss F, Lebrini M & Lagrenée M, ***Corros Sci***, 47 (2005) 2915.
20 Li W, He Q, Zhang S, Pei C & Hou B, ***J Appl Electrochem***, 38 (2008) 309.
21 Li X, Deng S & Fu H, ***Corros Sci***, 51 (2009) 1344.
22 Ferreira E S, Giacomelli C, Giacomelli F C & Spinelli A, ***Mater Chem Phys***, 83 (2004) 129.
23 Hassan H H, Abdelghani E & Amin M A, ***Electrochim Acta***, 52 (2007) 6359.
24 ***Abdel-Aal*** M S & ***Morad M S, Br Corros J***, 36 (2001) 253.
25 Bommersbach P, Alemany-Dumont C, Millet J P & Normand B, ***Electrochim Acta***, 51 (2005) 1076.
26 Mansfeld F, ***Corrosion***, 36 (1981) 301.
27 MaCafferty M & Hackerman N, ***J Electrochim Soc***, 119 (1972) 146.
28 El Azhar M, Mernari B, Traisnel M, Bentiss F & Lagrenée M, ***Corros Sci***, 43 (2001) 2229.
29 Haugstad G, ***Atomic Force Microscopy***: ***Understanding Basic Modes and Advanced Applications***, (John Wiley & Sons) 2012.
30 Kumar B R & Rao T S, ***Dig J Nanomater Bios***, 7 (4) (2012) 1881.